DESIGN AND OPTIMIZATION OF POROUS SNSE1-XSX NANOSHEETS USING HYDROTHERMAL REACTION

[1]HYUN JU, [2]JOOHEON KIM

[1,2]School of Chemical Engineering & Materials Science, Chung-AngUniversity, Seoul 06974, Republic of Korea Email:
E-mail: [1]mohani@cau.ac.kr, [2]jooheonkim@cau.ac.kr

Abstract - The introduction of a number of pores into the nanomaterials can manipulate their thermal transport characteristics of a material, which is considered as a promising strategy to improve the transport properties. Herein, we report on that the successful fabrication and optimization of porous SnSeS-based nanosheets. Two-dimensional $SnSe_{0.8}S_{0.2}$ (SnSeS) nanocrystals are chemically exfoliated from the layered bulk structure through a Li-intercalation and an exfoliation process. A large number of pores are successfully introduced into the SnSeS nanosheets through a solution-phase chemical transformation procedure, and the porosity of the materials can be optimized with different reaction time. The incorporation of nano and porous structure can boost the research advances regarding nano and porous materials.

Index Terms - Chalcogenides, Nanosheet, Porous material, Thermal conductivity

I. INTRODUCTION

Recently, it has reported that the SnSe has strong potential as an efficient thermoelectric material because of its extremely low thermal conductivity value originating from the strong anharmonicity of its chemical bonds [1,2]. However, the prospective study about the nanostructuring of SnSe-based materials to achieve the significant reduction of the thermal conductivity value have hardly been reported. Another powerful strategy for the lower thermal conductivity value is the introduction of nanoscale pores into the original structure. A lot of pores present in the materials can achieve dramatically low thermal conductivity arising from the phonon scattering at the porous boundaries [3,4].

Herein, we report on the preparation and optimization of porous $SnSe_{0.8}S_{0.2}$ (SnSeS) nanosheets by incorporation of the nanostructuring of SnSeS and introduction of pores on the nanostructure. The ternary SnSeS crystal have lower thermal conductivity value than the original SnSe because the substitution of isoelectric S atoms in the SnSe can cause atomic disorders that results in scattering positions of phonons [5]. A huge number of nano-sized pores are introduced into the prepared nanostructures via an organic acid-assisted chemical transformation reaction.We expect that the fabrication procedure can be applied to other porous nanomaterials in various research fields.

II. DETAILED EXPERIMENTS

Stoichiometric amounts of tin (Sn, 99.999%), selenium (Se, 99.999%), and sulfur (S, 99.999%) corresponding to the composition of $SnSe_{0.8}S_{0.2}$ (SnSeS) were loaded into quartz ampoule and then evacuated, which were subsequently sealed by a flame. The ampoule was slowly heated up to 1223 K in 10 h, and after holding the temperature for 6 h, the furnace was cooled to 298 K. The prepared ingot was ground into fine powder, and 0.5 g of SnSeS powder with a solution containing both 100 ml of ethylene glycol and 0.4 g of lithium hydroxide (LiOH) was added to a Teflon-lined autoclave. The autoclave was then heated to 473 K for 48 h to intercalate Li^+ ions into the layers of SnSeS. After that, the solution was cooled down naturally to 298 K. The resulting product was filtered and washed several times with acetone to eliminate any residual reactant, and then dried in a vacuum oven at 333 K for 24 h. After the procedure, 0.1 g of lithiated SnSeS powder was placed in a beaker filled with 40 ml of deionized (DI) water. The beaker was then sealed and sonicated at a low power for 1 h. After the resulting dispersion was centrifuged at 1000 rpm for 30 min, the supernatant was collected. The supernatant was then centrifuged at 8000 rpm for 30 min. The resulting product was purified several times with an aqueous HCl solution (3 vol.%). After washing the final product with ethanol several times, the SnSeS nanosheets were finally obtained after drying in a vacuum oven. 28.25 mg of resulting SnSeS nanosheets was added to an aqueous solution containing 225 mg of tartaric acid ($C_4H_6O_6$, t-acid) and 100 ml of DI water. After vigorous stirring, the mixture was then transferred into the Teflon-lined autoclave. The vessel was sealed and heated to 503 K for various reaction times (0, 1, 2, 4, 6, 9 hours) for the optimization of chemical transformation procedure. The resulting product was collected and washed with water and ethanol, and dried in a vacuum oven overnight.

III. RESULTS AND DISCUSSION

The SnSeS nanosheets with the stoichiometric composition of Sn, Se, and S (Sn:Se:S=1:0.8:0.2) were chemically exfoliated from the pulverized SnSeS powder that were prepared using the solid-state reaction and Li-intercalation process. Fig. 1a shows the X-ray diffraction (XRD) results of the pulverized SnSe and SnSeS powder, and exfoliated SnSeS nanosheets. The diffraction peaks of the SnSeS powder and

nanosheets have the same diffraction positions and they shifted slightly to the right compared to the SnSe powder, which is originated from the smaller anionic radius of S^{2-} (1.70 Å for S^{2-} and 1.84 Å for Se^{2-}) [6].

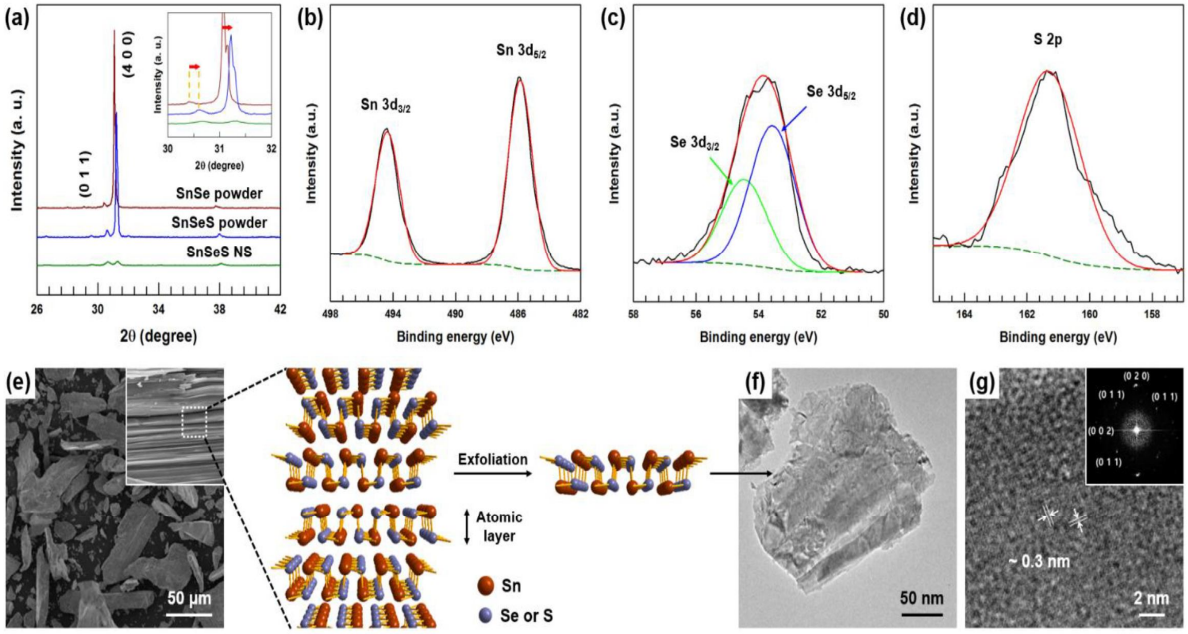


Fig. 1. (a) XRD results of the SnSe and SnSeS powder, and exfoliated SnSeS nanosheets.High-resolution XPS spectra of (b) Sn 3d, (c) Se 3d, and (d) S 2p of the SnSeS nanosheets. (e) FE-SEM image of the pulverized SnSeS powder. (f) Low- and (g) high-resolution FE-TEM images of the exfoliated SnSeS nanosheet. Schematic atomic structures are also provided in Figure 1e and 1f.

Fig.1b–d shows the high-resolution X-ray photoelectron spectroscopy (XPS) spectra of the Sn 3d, Se 3d, S 2p binding energies of SnSeS, respectively. The peaks at ~494.2 and 485.7 eV in the Sn 3d region are corresponded to the Sn $3d_{3/2}$ and Sn $3d_{5/2}$ binding energies, while the Se $3d_{3/2}$ and Se $3d_{5/2}$ peaks are shown at about 54.3 and 53.4 eV. In case of the S $2p_{3/2}$ peak, it is located at ~161 eV. The measured binding energies of the SnSeS are close to those in the previously reported binding energies for Sn^{2+}, Se^{2-}, and S^{2-} [7], whose results also prove the successful fabrication of the SnSeS nanosheets. The field-emission scanning electron microscopy(FE-SEM) and field-emission transmission electron microscopy (FE-TEM) images further confirmed the microstructural details of the fabricated SnSeS materials. Fig. 1e shows the FE-SEM image of the pulverized SnSeS powder, exhibiting the layered internal structures in the inset. The exfoliated SnSeS nanosheet is clearly observed in the low-resolution FE-TEM image in the Fig. 1f, which shows the sheet-like structures with size of approximately 200 nm. The high-resolution FE-TEM image (Fig. 1g) denotes the lattice spacing of ~0.3 nm, corresponding to the (0 0 1) plane of SnSeS. On the basis of the above results, the fabricated SnSeS nanosheets were successfully characterized.

In order to introduce lots of pores into the SnSeS nanosheets, the aqueous solution consisting of the SnSeS nanosheets and tartaric acid (t-acid, $C_4H_6O_6$) was hydrothermally reacted for the chemical transformation of the SnSeS. The t-acid dissolved the Sn^{2+} ions in the SnSeS nanosheets through the formation of Sn(t-acid), and the depleting sites were transformed to pores, leading to the fabrication of the porous SnSeS nanosheets. The Sn(t-acid) could be soluble in the water, as previously found for Sb ions of Sb_2Te_3 with t-acid in aqueous solution [8]. In parallel, the Se^{2-} and S^{2-} ions were oxidized by O_2 to Se^0 and S^0.This reaction mechanism is schematically proposed in the Fig. 2a and 2b, and also described in equation (1) and (2).

$$SnSeS + C_4H_6O_6 \rightarrow Sn^{2+}(C_4H_4O_6)^{2-} + 0.8\,Se^{2-} + 0.2\,S^{2-} + 2\,H^+ \quad (1)$$

$$0.8\,Se^{2-} + 0.2\,S^{2-} + 0.5\,O_2 + H_2O \rightarrow 0.8\,Se + 0.2\,S + 2\,OH^- \quad (2)$$

Theporous SnSeS nanosheets were successfully obtained via the solution-phase chemical transformation procedure described above. After the preparation of the porous SnSeS nanosheets, XRD analysis was firstly performed to investigate the crystalline phases of the materials. Fig. 3a shows the resulting XRD patterns of the porous SnSeS nanosheets with different reaction times. All samples consist only of the diffraction peaks that are the same positions compared to the result of the SnSeS nanosheets shown in Fig. 1a, implying that there were no other materials except SnSeS

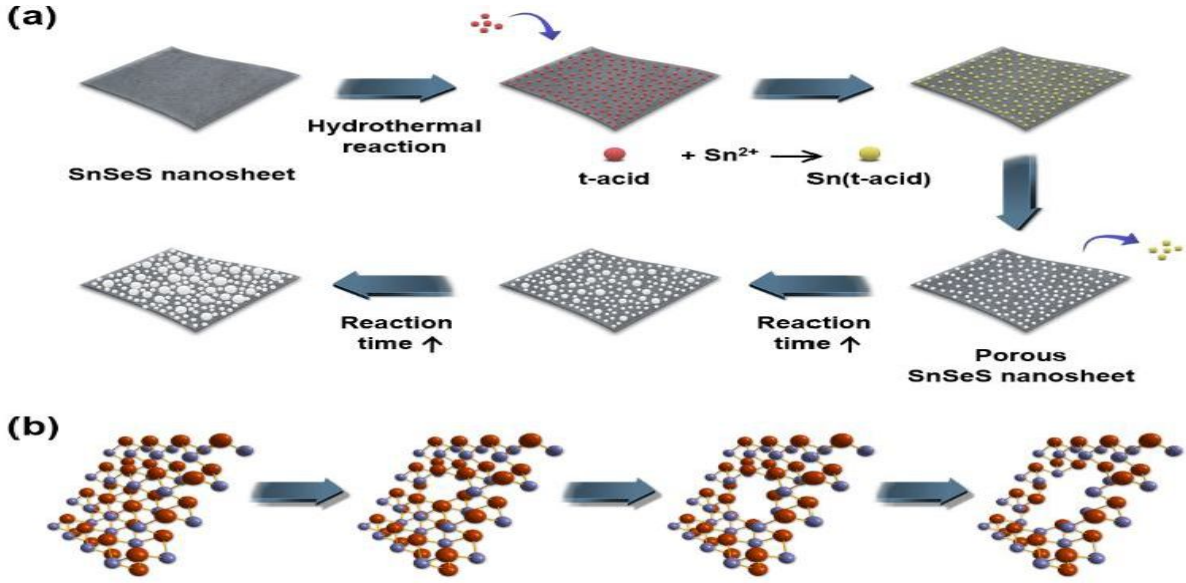


Fig. 1. (a) Schematic representation and (b) the detailed mechanism of the chemical transformation process for the porous SnSeS nanosheet.

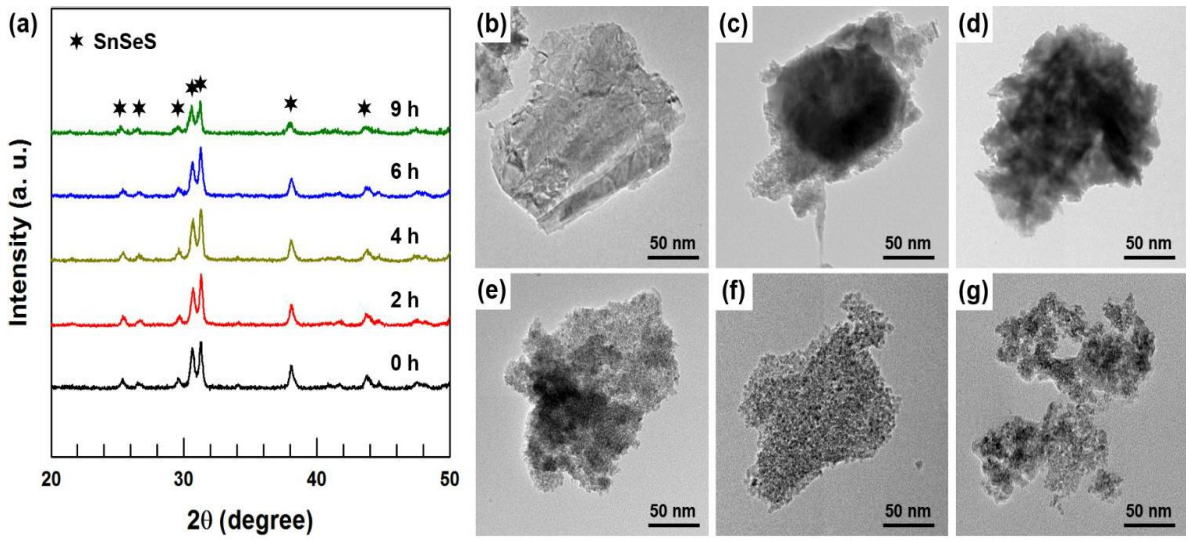


Fig. 3. (a) XRD patterns of porous SnSeS nanosheets with different reaction times. FE-TEM images for the porous SnSeS nanosheets at the reaction time of (b) 0, (c) 1, (d) 2, (e) 4, (f) 6, and (g) 9 h.

in the samples. This result is attributed to that the reduced Se and S crystals were melted out from the surface of the SnSeS nanosheets because the reaction temperature (503 K) is higher than the melting points of Se (494 K) and S (388 K). FE-TEM images clearly revealed that the reaction time is a critical factor to determine the porous morphology of the products. Fig. 3b–g shows the FE-TEM images of the porous SnSeS nanosheets with increasing reaction times. As the reaction time increased, the surface of the SnSeS nanosheet became rough, and then the numerous pores were introduced on the surface of the sample. The prolonged reaction time resulted in the generation of larger pores on the surface of the SnSeS nanosheet. In case of the sample processed for 9h(Fig. 3g) presents that the generated pores broke the sheet-like morphology. This result is in agreement with the schematic representation shown in Fig. 2.

CONCLUSION

Two-dimensional SnSeS nanocrystals were chemically exfoliated from the layered bulk structure through a Li-intercalation and an exfoliation process. The resulting SnSeS particles had sheet-like structures with size of ~200 nm. A large number of pores were successfully introduced into the SnSeS nanosheets through a solution-phase chemical transformation procedure in the presence of the t-acid which dissolved the Sn ions from the SnSeS, and the depleting positions were transformed to pores, resulting in the porous SnSeS nanosheets.During the reaction process, the reaction time was a crucial factor to determine the porous morphology of the products. The surface of the SnSeS nanosheet became rough as the reaction time increased, and a great number of pores were generated on the surface of the sample after the prolonged

reaction time.The incorporation of nano and porous structure in this work can be widely applied to other researches for nano and porous materials.

REFERENCES

[1] L.-D. Zhao, S.-H. Lo, Y. Zhang, H. Sun, G. Tan, C. Uher, C. Wolverton, V.P. Dravid, and M.G. Kanatzidis, "Ultralow thermal conductivity and high thermoelectric figure of merit in SnSe crystals," Nature, vol. 508, pp. 373-377, Apr.2014.

[2] C.W. Li, J. Hong, A.F. May, D. Bansal, S. Chi, T. Hong, G. Ehlers, and O. Delaire, "Orbitally driven giant phonon anharmonicity in SnSe," Nat. Phys., vol. 11, pp. 1063-1069, Oct. 2015.

[3] Y. Zhang, T. Day, M.L. Snedaker, H. Wang, S. Krämer, C.S. Birkel, X. Ji, D. Liu, G.J. Snyder, and G.D. Stucky, "A mesoporous anisotropic n-Type Bi_2Te_3 monolith with low thermal conductivity as an efficient thermoelectric material," Adv. Mater., vol. 24, pp. 5065-5070, Jul. 2012.

[4] X. Chen, A. Weathers, A. Moore, J. Zhou, and L. Shi, "Thermoelectric properties of cold-pressed higher manganese silicides for waste heat recovery," J. Electron. Mater., vol. 41, pp. 1564-1572, Mar. 2012.

[5] M. Hong, T.C. Chasapis, Z.-G. Chen, L. Yang, M.G. Kanatzidis, G.J. Snyder, and J. Zou, "n-Type $Bi_2Te_{3-x}Se_x$ nanoplates with enhanced thermoelectric efficiency driven by wide-frequency phonon scatterings and synergistic carrier scatterings," ACS Nano, vol. 10, pp. 4719-4727, Apr. 2016.

[6] R.t. Shannon, "Revised effective ionic radii and systematic studies of interatomic distances in halides and chalcogenides," Acta Crystallogr., Sect. A: Cryst. Phys., Diffr., Theor. Gen. Crystallogr., vol. 32, pp. 751-767, Mar. 1976.

[7] M.A. Franzman, C.W. Schlenker, M.E. Thompson, and R.L. Brutchey, "Solution-phase synthesis of SnSe nanocrystals for use in solar cells," J. Am. Chem. Soc., vol. 132, pp. 4060-4061, Mar. 2010.

[8] H. Zhang, H. Wang, Y. Xu, S. Zhuo, Y. Yu, and B. Zhang, "Conversion of Sb_2Te_3 hexagonal nanoplates into three-dimensional porous single-crystal-like network-structured Te plates using oxygen and tartaric acid," Angew. Chem. Int. Ed., vol. 51, pp. 7-782, May 2001.

